Hypocretin (Orexin) Receptor Subtypes Differentially Enhance Acetylcholine Release and Activate G Protein Subtypes in Rat Pontine Reticular Formation

René Bernard, Ralph Lydic, and Helen A. Baghdoyan

Departments of Anesthesiology (RB, RL, HAB) and Pharmacology (RB, HAB)

University of Michigan, Ann Arbor, MI 48109

JPET Fast Forward. Published on December 13, 2005 as DOI: 10.1124/jpet.105.097071
This article has not been copyedited and formatted. The final version may differ from this version.

a) Running title: Hcrt receptors increase ACh release and activate G proteins

b) Corresponding author:
Helen A. Baghdoyan, Ph.D.
University of Michigan
Department of Anesthesiology
7433 Medical Sciences Building I
1150 West Medical Center Drive
Ann Arbor, Michigan 48109-0615
Voice: (734) 647-7831
Fax: (734) 764-9332
Email: helenb@umich.edu

c) Number of:
text pages = 37
tables = 0
figures = 6
references = 53
words in the Abstract = 243
words in the Introduction = 494
words in the Discussion = 1413

d) Nonstandard abbreviations:

ACh, acetylcholine; ANOVA, analysis of variance; DAMGO, [D-Ala2, N-Me-Phe4, Gly5] enkephalin; EGTA, ethylene glycol bis(2-aminoethyl ether) tetraacetic acid; GABA, gamma amino butyric acid; GDP, guanosine 5'-diphosphate; [^{35}S]GTPγS, [^{35}S]guanylyl-5'-O-(γ-thio)triphosphate; hcrt, hypocretin; hcrt-r1, hypocretin receptor subtype 1; hcrt-r2, hypocretin receptor subtype 2; PnO, pontine reticular nucleus oral part; PTX, pertussis toxin; REM, rapid eye movement; SPA, N^6-*p*-sulfophenyladenosine; VEH, vehicle

e) Recommended section assignment: Neuropharmacology

Abstract

The hypothalamic peptides hypocretin-1 (orexin A) and hypocretin-2 (orexin B) promote wakefulness by mechanisms that are not well understood. Defects in hypocretinergic neurotransmission underlie the human sleep disorder narcolepsy. Hypocretins alter cell excitability via two receptor subtypes, hcrt-r1 and hcrt-r2. This study aimed to identify G protein subtypes activated by hypocretin in the oral part of rat pontine reticular nucleus (PnO), and the hypocretin receptor subtype modulating acetylcholine (ACh) release in the PnO. G protein activation was quantified using in vitro [^{35}S]GTPγS autoradiography. ACh release was measured using in vivo microdialysis and high performance liquid chromatography. Hypocretin-1-stimulated G protein activation was significantly decreased by pertussis toxin, demonstrating that some hypocretin receptors in rat PnO activate inhibitory G proteins. Hypocretin-1-stimulated ACh release was not blocked by pertussis toxin, supporting the conclusion that the hypocretin receptors modulating ACh release in rat PnO activate stimulatory G proteins. Hypocretin-1 and hypocretin-2 each caused a concentration dependent increase in ACh release with similar potencies, indicating that hcrt-r2 modulates ACh release in PnO. Hypocretin-1 caused a significantly greater increase in ACh release than hypocretin-2, suggesting a role for hcrt-r1 in the modulation of PnO ACh release. Taken together, these data provide the first evidence that hypocretin receptors in rat PnO signal via inhibitory and stimulatory G proteins, and that ACh release in rat PnO is modulated by hcrt-r2 and hcrt-r1. One mechanism by which hypocretin promotes arousal may be to increase ACh release in the pontine reticular formation.

Introduction

Hypocretin-1 and hypocretin-2 (orexin A and orexin B) are neuropeptides synthesized by a small group of lateral hypothalamic neurons that project extensively throughout the brain (de Lecea et al., 1998; Peyron et al., 1998; Sakurai et al., 1998). Physiological roles of the hypocretin peptides include promoting behavioral arousal and locomotor activity, as well as modulating food intake and energy homeostasis (Kukkonen et al., 2002; Smart and Jerman, 2002). Impaired hypocretinergic signaling underlies the human sleep disorder narcolepsy (Nishino et al., 2000; Thannickal et al., 2000), and defects in hypocretin peptides or receptors produce animal models of narcolepsy (Chemelli et al., 1999; Lin et al., 1999). The mechanisms by which hypocretins modulate arousal are not well understood, and may include excitation (de Lecea et al., 1998) of brainstem neurons that promote behavioral arousal and cortical activation (Kilduff and Peyron, 2000). Hypocretinergic neurons discharge at their fastest rates during active wakefulness (Lee et al., 2005; Mileykovskiy et al., 2005), and hypocretins have excitatory effects on noradrenergic neurons of the locus coeruleus, serotonergic neurons of the dorsal raphe, and cholinergic neurons of the laterodorsal and pedunculopontine tegmental nuclei (reviewed in Kukkonen et al., 2002).

Hypocretin-1 and hypocretin-2 alter cell excitability via two receptor subtypes (hcrt-r1 and hcrt-r2) (Sakurai et al., 1998). Hypocretin-1 has relatively high affinity for both receptor subtypes, whereas hypocretin-2 has higher affinity for hcrt-r2 than for hcrt-r1 (Sakurai et al., 1998; Smart et al., 2001). Both hypocretin receptor subtypes couple to guanine nucleotide binding (G) proteins (Sakurai et al., 1998). Pertussis toxin is a standard pharmacological tool for blocking signal transduction mediated by inhibitory G proteins (Carty, 1994), and work with in vitro expression systems has shown that hcrt-r2 couples to both pertussis toxin-insensitive and

pertussis toxin-sensitive G proteins (Zhu et al., 2003). The G protein subtypes coupled to each hypocretin receptor subtype in vivo remain to be determined, and may vary across brain regions.

The present study focused on functional effects of hypocretin in one arousal promoting brainstem region, the oral part of the pontine reticular nucleus (PnO). The PnO is the rostral portion of rat pontine reticular formation (Paxinos and Watson, 1998). In vivo and in vitro approaches were combined with the goal of identifying mechanisms by which the arousal promoting peptide hypocretin acts within the PnO, which comprises an important part of the ascending reticular activating system. In vitro autoradiography was used to test the hypothesis that treatment of the PnO with pertussis toxin inhibits hypocretin-1-stimulated [^{35}S]GTPγS binding in PnO. A second series of experiments utilized in vivo microdialysis to test the hypothesis that treatment of the PnO with pertussis toxin inhibits hypocretin-1-stimulated ACh release in PnO. Finally, in vivo microdialysis was used to test the hypothesis that hypocretin-1 and hypocretin-2 each cause a concentration dependent increase in PnO ACh release. The concentration response curves for hypocretin-1- and hypocretin-2-stimulated ACh release were compared with the goal of identifying the hypocretin receptor subtype modulating ACh release in the PnO.

Materials and Methods

Animals. Adult, male Crl:CD®(SD)IGS BR (Sprague Dawley) rats (250-350 g) were purchased from Charles River Laboratories (Wilmington, MA) and housed in a 12:12 h light/dark cycle for at least one week prior to use. Experiments were conducted in accordance with the *Guide for the Care and Use of Laboratory Animals* (National Academy Press, Washington, DC, 1996) and with approval by the University of Michigan Committee on Use and Care of Animals. All in vivo experiments were performed under general anesthesia using the following procedure. A rat was placed in a Plexiglas chamber and anesthesia was induced with isoflurane (2-3 % in 100% O_2). The anesthetized rat then was placed in a stereotaxic frame (David Kopf, Tujunga, CA) and isoflurane was delivered through a rat anesthesia mask (David Kopf) using a flow rate of 0.6 L O_2/min. Delivered isoflurane levels were measured continuously with an infrared gas analyzer (Cardiocap™/5, Datex-Ohmeda, Louisville, CO) and held at 1.5% throughout the experiment. A re-circulating heat pump (Gaymar Industries, Orchard Park, NY) was used to maintain core body temperature at 37ºC. Using a Dremel (Racine, WI), a small hole was made in the skull to permit unilateral access to the PnO according to a rat brain atlas (Paxinos and Watson, 1998). Stereotaxic coordinates for the PnO were 8.6 mm posterior to bregma, 1.2 mm from the midline, and 9.2 mm ventral to the skull surface. Animals were kept warm and observed continuously during recovery from anesthesia.

Chemicals, Materials, and Microdialysis Probes. Hypocretin-1 (human, rat, mouse) was purchased from California Peptide Research (Napa, CA). Hypocretin-2 (rat, mouse) was obtained from AnaSpec, Inc. (San Jose, CA). Pertussis toxin was obtained from Sigma-Aldrich

(St. Louis, MO) and List Biological Laboratories (Campbell, CA). [D-Ala2, N-Me-Phe4, Gly5] enkephalin (DAMGO), guanosine 5'-diphosphate (GDP), guanosine 5'-O-(γ-thio)triphosphate (GTPγS), N^6-*p*-sulfophenyladenosine (SPA) and all other chemicals were purchased from Sigma-Aldrich (St. Louis, MO). Reflection autoradiography film (Kodak X-OMAT Blue XB-1) and [^{35}S]guanylyl-5'-O-(γ-thio)triphosphate ([^{35}S]GTPγS) were obtained from Perkin Elmer Life Science Products (Boston, MA).

CMA/11 microdialysis probes (Cuprophane membrane: l mm long, 0.24 mm in diameter, 6 kDa cut-off; CMA Microdialysis, North Chelmsford, MA) were used for drug delivery to the PnO and for simultaneous collection of endogenous ACh. Probes were connected to a CMA/100 pump that delivered a constant 2.0 μl/min flow rate. Dialysis probes were perfused continuously with Ringer's solution (147 mM NaCl, 4.0 mM KCl, 2.4 mM $CaCl_2$, 10 μM neostigmine bromide, pH 5.8 to 6.2). All drugs delivered by microdialysis were dissolved in Ringer's solution.

Quantification of ACh using high performance liquid chromatography with electrochemical detection (HPLC-ECD). Dialysis samples were injected manually into an HPLC-ECD system (Bioanalytical Systems (BAS), West Lafayette, IN) that separated ACh and choline and converted ACh into hydrogen peroxide. Electrochemically active hydrogen peroxide was detected by a platinum electrode and generated a chromatogram that was stored digitally and analyzed using ChromGraph® software (BAS). ACh chromatograms generated by dialysis samples were compared to a standard curve produced from known amounts of ACh (0.05 to 1 pmol). A standard curve was generated before every experiment. ACh was quantified as pmol/15 min.

Before each experiment, a dialysis probe was placed into a solution of known ACh concentration. Five 30 µl samples were collected and analyzed for ACh to calculate percent of ACh recovered by the probe. At the end of each dialysis experiment, the dialysis probe was removed from the brain and placed again in a solution of known ACh concentration to collect an additional five 30 µl samples for calculating percent recovery of ACh. Pre-and post-experimental probe recoveries were compared by t-test. The present study includes data from experiments in which probe recoveries did not change significantly in the direction of the hypothesized drug effect. This procedure ensured that measured changes in ACh resulted from drug effects and were not an artifact of intra-experimental changes in dialysis membrane properties.

Histological localization of dialysis sites. Two to three days following each dialysis experiment, animals were deeply anesthetized and decapitated. The brainstem was cut serially to obtain 40 µm thick coronal sections through the pontine reticular formation. Tissue sections were mounted on chrome alum coated slides, fixed in paraformaldehyde vapor (80°C), and stained with cresyl violet. Stained sections were digitized using a Cohu CCD camera with a Micro Nikon 60 mm objective, the Scion Image 1.62c version of NIH Image, and a G3 Apple Macintosh computer. Stereotaxic coordinates were assigned to each dialysis probe site by comparing the digitized images and actual tissue sections to the plates in a rat brain atlas (Paxinos and Watson, 1998).

Methods for testing the hypothesis that pertussis toxin blocks hypocretin-1-stimulated G protein activation: in vivo pertussis toxin microinjection followed by in vitro [^{35}S]GTPγS autoradiography. Pertussis toxin was administered to intact animals by microinjection into the PnO before brain removal and sectioning. To perform an in vivo microinjection, rats were anesthetized as described above and a stainless steel guide tube was aimed stereotaxically for the PnO. A stainless steel microinjector was inserted through the guide tube and pertussis toxin (0.25 μg/0.25μl) was delivered to the PnO. Control rats received a unilateral PnO microinjection (0.25 μl) of vehicle solution consisting of 0.1 M sodium phosphate buffer and 0.5 M sodium hydroxide. Rats were decapitated 48 h post-injection when ADP-ribosylation of G proteins is nearly complete (van der Ploeg et al., 1991). Brains were frozen in a bilayer composed of bromobutane and isopentane (-30ºC) and the pons was sectioned coronally from bregma -8.80 to -7.30 mm (Paxinos and Watson, 1998) using a Leica CM3050 S cryostat (Leica Microsystems, Nussloch, Germany). Serial sections were thaw-mounted pair-wise onto chrome alum coated slides. Slide mounted tissue sections were dried in a desiccator (4ºC) for 2 hours, then stored at -80°C until used for [^{35}S]GTPγS autoradiography.

The binding assay for in vitro [^{35}S]GTPγS autoradiography has been described previously (Bernard et al., 2003). Assay buffer contained 50 mM Tris-HCl, 3 mM $MgCl_2$, 0.2 mM EGTA, and 100 mM NaCl (pH 7.4). Slide mounted tissue sections were brought to room temperature and incubated for 2 h in assay buffer containing 0.04 nM [^{35}S]GTPγS and 2 mM GDP and one of the following four treatment conditions: hypocretin-1 (200 nM), DAMGO (3 μM) as a positive control, unlabeled GTPγS (10 μM) for non-specific binding, or basal [^{35}S]GTPγS binding in the absence of exogenous ligands. The incubation period was terminated by rinsing the tissue sections in ice-cold 50 mM Tris-HCl buffer (pH 7.0) followed by ice-cold deionized water.

Sections were dried overnight and placed in lightproof stainless steel cassettes (Fisher Scientific, Pittsburg, PA) along with ^{14}C microscale standards (31-883 nCi/g, Amersham Biosciences, Arlington Heights, IL) and X-OMAT Blue XB-1 film (Eastman Kodak Company, Rochester, NY). After a 72-h exposure period, films were developed with a Kodak X-OMAT Model 2002A film processor. Tissue sections were fixed and stained with cresyl violet, and autoradiograms and stained tissue sections were digitized as described above.

The PnO is a bilateral structure and [^{35}S]GTPγS binding was measured on both the injected and non-injected side of the PnO for rats microinjected with pertussis toxin and rats microinjected with vehicle. The PnO was identified on the cresyl violet stained tissue sections according to a rat brain atlas (Paxinos and Watson, 1998). A digital outline of the PnO was transferred to the matching position in each autoradiogram and optical density was quantified. Optical density measures were converted to total [^{35}S]GTPγS binding (nCi/g) using a ^{14}C standard curve and a ^{14}C correction factor for ^{35}S. Specific PnO [^{35}S]GTPγS binding was obtained by subtracting the mean non-specific binding value for the PnO from every individual total [^{35}S]GTPγS binding measurement. Individual specific [^{35}S]GTPγS binding measures were averaged by treatment condition for each animal. Data were analyzed using descriptive statistics, one-way analysis of variance (ANOVA) for repeated measures, and Tukey/Kramer multiple comparisons test (GB-Stat ^{TM} v 6.5.6 Dynamic Microsystems, Inc., Silver Spring, MD). The alpha level was set at $p<0.05$, and power calculations were performed to ensure using the smallest number of animals required to achieve a beta level of 80%.

JPET Fast Forward. Published on December 13, 2005 as DOI: 10.1124/jpet.105.097071
This article has not been copyedited and formatted. The final version may differ from this version.

Methods for testing the hypothesis that pretreatment of the PnO with pertussis toxin inhibits hypocretin-1-stimulated ACh release in the PnO: in vivo microinjection followed by in vivo microdialysis. Animals were surgically prepared with guide tubes aimed for the PnO and microinjected with pertussis toxin or pertussis toxin vehicle as described above. Forty-eight h after pertussis toxin administration, rats were anesthetized with isoflurane and a dialysis probe was placed through the guide tube into the PnO. Dialysis samples (30 μl) were collected every 15 min. Five samples were collected during dialysis with Ringer's to establish baseline levels of ACh release. A CMA/110 liquid switch then was turned to deliver Ringer's containing hypocretin-1 (100 μM) to the probe. Five sequential dialysis samples were collected during continuous PnO administration of hypocretin-1. The probe then was removed from the brain. Brainstems were processed for cresyl violet histology, as described above.

Positive control experiments were performed using dialysis administration of the adenosine A_1 receptor agonist SPA (300 μM). Adenosine A_1 receptors couple to pertussis toxin-sensitive G proteins (Ribeiro et al., 2003) and SPA decreases ACh release in cat pontine reticular formation (Tanase et al., 2003). Thus, pretreatment with pertussis toxin was predicted to inhibit the SPA-induced decrease in ACh release, and pretreatment with pertussis toxin vehicle was predicted to have no effect on the SPA-induced decrease in ACh release.

ACh release during dialysis administration of hypocretin-1 or SPA was expressed as a percent of baseline ACh measured during dialysis with Ringer's for each experiment. Data were analyzed by descriptive statistics and two-way ANOVA (Statistical Analysis System (SAS) software, release 9.1.2, SAS Institute, Inc., Cary, NC). A significant ANOVA was followed by a Tukey/Kramer multiple comparisons test. The alpha level for statistical significance was set at

$p<0.05$. Power calculations ascertained that all analyses used the minimum number of animals needed to achieve a beta level of 80%.

Methods for testing the hypothesis that hypocretin-1 and hypocretin-2 each cause a concentration dependent enhancement of ACh release in the PnO: in vivo microdialysis. Animals were anesthetized as described above and a dialysis probe was aimed unilaterally for the PnO. No microinjections were made before dialysis for these studies. Five control samples (75 min) were collected during dialysis with Ringer's before hypocretin-1 or hypocretin-2 delivery was initiated by turning a CMA/110 liquid switch. Four concentrations of hypocretin-1 and hypocretin-2 (0.1, 1, 10, and 100 μM) were use. Each rat was used for only one experiment, and only one concentration of hypocretin was tested per experiment. Five dialysis samples (75 min) were collected during continuous hypocretin delivery. When the last dialysis sample was collected, the probe was removed from the brain, the scalp was closed, and the animal recovered from anesthesia. Brains were processed for cresyl violet histology two to three days later, as described above.

Data were analyzed using descriptive and inferential statistics. The alpha level for statistical significance was set at $p<0.05$. The smallest number of animals required to achieve a beta level of 80% was established using power calculations. One-way ANOVA and Dunnett's multiple comparisons test (GB-Stat) were used to determine if each peptide concentration significantly increased ACh release. Non-linear regression analysis (GraphPad Prism software v4.0a for Macintosh, GraphPad Software Inc., San Diego, CA) was used to fit sigmoid curves to the concentration response data according to the following equation: % of Ringer's ACh release = Basal % Ringer's release + (Maximum % Ringer's release - Basal % Ringer's release) / 1+10

$^{(\log EC50-X)}$, where X is the logarithm of the concentration of hypocretin-1 or hypocretin-2. Regression analyses provided the coefficient of determination (r^2) for each of the peptides, as well as the concentration of hypocretin-1 and hypocretin-2 that produced a half-maximal increase ACh release (EC_{50}). Two-way ANOVA for repeated measures (SAS) was used to compare the concentration response curves for ACh release stimulated by hypocretin-1 and hypocretin-2. Bonferroni post hoc tests identified statistically significant differences in ACh release caused by equimolar concentrations of hypocretin-1 and hypocretin-2.

JPET Fast Forward. Published on December 13, 2005 as DOI: 10.1124/jpet.105.097071
This article has not been copyedited and formatted. The final version may differ from this version.

Results

Hypocretin-1-stimulated [^{35}S]GTPγS binding was inhibited by pertussis toxin.

Figure 1 summarizes the results of experiments testing the hypothesis that pertussis toxin inhibits hypocretin-1-stimulated G protein activation. Pertussis toxin (Fig. 1A) or vehicle solution (Fig. 1D) were microinjected into one side of the PnO 48 h before brain removal for autoradiography. The contralateral side of the PnO served as the non-injected control. Figs. 1B, 1C, 1E, and 1F summarize the results of the quantitative autoradiography. The total number of [^{35}S]GTPγS binding measurements contributing to each figure is reported below. In order to avoid inflated degrees of freedom for statistical analyses measurements were averaged by rat. This resulted in a sample size of N=4 as shown in Figs. 1B and 1C, and N=3 in Figs. 1E and 1F.

Figure 1B plots basal and hypocretin-1-stimulated specific [^{35}S]GTPγS binding on the non-injected and pertussis toxin-injected sides of the PnO. Results are based on 386 measurements from four rats. ANOVA revealed a significant ($F=19.5$; $df=3,12$; $p<0.001$) treatment main-effect on [^{35}S]GTPγS binding. On the non-injected side of the PnO, hypocretin-1 significantly ($p<0.01$) increased [^{35}S]GTPγS binding over basal levels (28.9%). In contrast, on the pertussis toxin-injected side of the PnO hypocretin-1 did not significantly increase [^{35}S]GTPγS binding over basal levels. On the pertussis toxin-injected side of the PnO, hypocretin-1-stimulated [^{35}S]GTPγS binding was significantly ($p<0.01$) lower (-25.1%) than on the non-injected side of the PnO.

Figure 1C illustrates the results of positive control experiments that used the mu opioid receptor agonist DAMGO to stimulate [^{35}S]GTPγS binding. Results are based on 384 measurements from four rats. Repeated measures ANOVA revealed a significant ($F=42.3$; $df=3,12$; $p<0.0001$) treatment main-effect on [^{35}S]GTPγS binding. On the non-injected side of

the PnO, DAMGO significantly ($p<0.01$) increased [^{35}S]GTPγS binding (95.6%) over basal levels. On the pertussis toxin-injected side of the PnO, the DAMGO-stimulated increase (49.6%) in [^{35}S]GTPγS binding was significantly ($p<0.01$) decreased (-37.3%) below the DAMGO-stimulated increase on the contralateral, non-injected PnO.

Additional control experiments involved unilateral microinjection of the pertussis toxin vehicle into the PnO 48 h before brain removal for autoradiography (Fig. 1D). Figure 1E summarizes the effects of vehicle microinjection on basal and hypocretin-1-stimulated [^{35}S]GTPγS binding. Results are based on 339 measurements from three rats. Repeated measures ANOVA showed a significant ($F=22.7$; $df=2,9$; $p<0.001$) treatment main-effect on [^{35}S]GTPγS binding. On the non-injected side of the PnO, [^{35}S]GTPγS binding was significantly ($p<0.01$) increased over basal levels by hypocretin-1 (19.7%). On the side of the PnO that received a vehicle microinjection, hypocretin-1-stimulated [^{35}S]GTPγS binding also was significantly ($p<0.01$) increased (18.7%) over basal binding. Specific [^{35}S]GTPγS binding levels for basal and hypocretin-1-treated sections on the non-injected side of the PnO were not different from binding levels of the corresponding treatment conditions on the vehicle-microinjected side of the PnO.

Figure 1F shows the effects of vehicle microinjection on basal and DAMGO-stimulated [^{35}S]GTPγS binding in the PnO. Results are based on 340 measurements from three rats. Repeated measures ANOVA revealed a significant ($F=182.9$; $df=2,9$; $p<0.0001$) treatment main-effect on [^{35}S]GTPγS binding. On the non-injected side of the PnO, [^{35}S]GTPγS binding was significantly ($p<0.01$) increased over basal levels by DAMGO (82.6%). On the vehicle-injected side of the PnO, DAMGO-stimulated [^{35}S]GTPγS binding also was significantly ($p<0.01$) increased (81.0%) over basal binding. Specific [^{35}S]GTPγS binding levels for basal and

DAMGO-treated sections on the non-injected side of the PnO were not different from binding levels of the corresponding treatment conditions on the vehicle-microinjected side of the PnO.

The stereotaxic coordinates of histologically localized microinjection sites (Figs. 1A and 1D) were compared using the Bonferroni t-test. Mean ± s.e.m. stereotaxic coordinates for pertussis toxin injection sites (8.54 ± 0.18 mm posterior to bregma; 1.61 ± 0.07 mm lateral to bregma; 8.50 ± 0.04 mm ventral to bregma) were not significantly different from the stereotaxic coordinates for vehicle microinjection sites (8.34 ± 0.21 mm posterior to bregma; 1.48 ± 0.16 mm lateral to bregma; 8.47 ± 0.09 mm ventral to bregma).

Pertussis toxin did not inhibit hypocretin-1-stimulated ACh release. Figure 2 localizes the microdialysis sites used to test the hypothesis that pretreatment with pertussis toxin blocks hypocretin-1-stimulated ACh release. All probe sites were located in the PnO. Bonferroni t-test revealed that the average ± s.e.m. stereotaxic coordinates for pertussis toxin injection sites (8.04 ± 0.11 mm posterior to bregma; 1.38 ± 0.07 mm lateral to bregma; 9.18 ± 0.12 mm ventral to bregma) were not significantly different from the stereotaxic coordinates for vehicle injection sites (8.13 ± 0.06 mm posterior to bregma; 1.18±0.04 mm lateral to bregma; 9.13 ± 0.10 mm ventral to bregma).

The effects of pertussis toxin or vehicle pretreatment on hypocretin-1-stimulated ACh release were tested in six experiments summarized by Fig. 3A. Two way ANOVA was based on 60 dialysis samples, accounted for as follows: 5 samples per dialysis condition x 2 dialysis conditions (Ringer's vs. hypocretin-1) x 2 pretreatment conditions (vehicle injection vs. pertussis toxin injection) x 3 rats per pretreatment condition. There was a significant effect of dialysis condition (Ringer's vs. hypocretin-1) on ACh release ($F=176.6$; $df=1,52$; $p<0.0001$), no

significant effect of pretreatment (vehicle vs. pertussis toxin), and no significant interaction. Hypocretin-1 significantly ($p<0.0001$) increased ACh release in the PnO after microinjection of vehicle (67.1%) and after microinjection of pertussis toxin (54.6%). ACh levels were not different between pertussis toxin and vehicle injected rats. Mean ± s.e.m. basal (Ringer's) ACh levels (pmol/15 min) were 0.077 ± 0.006 for vehicle injection experiments and 0.086 ± 0.005 for pertussis toxin injection experiments (Fig. 3A).

The adenosine A_1 receptor agonist SPA served as a positive control for the effects of pertussis toxin. Figure 3B illustrates results from six rats (n=60 dialysis samples) that underwent dialysis administration of SPA following pretreatment with pertussis toxin or vehicle. Two-way ANOVA showed a significant effect of dialysis condition (Ringer's vs. SPA) on ACh release ($F=17.5$; $df=1,52$; $p<0.0001$), a significant effect of pretreatment (vehicle vs. pertussis toxin) on ACh release ($F=10.6$; $df=1,4$; $p=0.03$), and a significant interaction ($F=10.6$; $df=1,52$; $p=0.002$). SPA significantly ($p<0.0001$) decreased (-30.7%) ACh release in the PnO after vehicle microinjection. The SPA-induced decrease in ACh release was blocked by pretreatment with pertussis toxin. SPA-stimulated ACh release after vehicle microinjection was significantly ($p=0.0002$) lower (-28.0%) than SPA-stimulated ACh release following pertussis toxin microinjection. Mean ± s.e.m. basal (Ringer's) ACh levels (pmol/15 min) were 0.081 ± 0.005 for vehicle injection experiments and 0.123 ± 0.006 for pertussis toxin injection experiments (Fig. 3B).

Hypocretin-1 and hypocretin-2 each caused a concentration dependent increase in ACh release. Figure 4 summarizes the location of all dialysis sites used for the concentration response studies. Figure 4A shows representative histological sections from a rat that received

hypocretin-1 (left) and a rat that received hypocretin-2 (right). Histological analysis of all hypocretin-1 (Fig. 4B) and hypocretin-2 (Fig. 4C) dialysis sites confirmed that measures of ACh were obtained from the PnO. Analysis of the stereotaxic coordinates for the dialysis sites determined that mean ± s.e.m. probe sites for hypocretin-1 delivery (8.00 ± 0.07 mm posterior to bregma; 1.30 ± 0.06 mm lateral to bregma; 8.98 ± 0.05 mm ventral to bregma; N=12 experiments) were not significantly different from probe sites for hypocretin-2 delivery (8.30 ± 0.11 mm posterior to bregma; 1.33 ± 0.07 mm lateral to bregma;8.98 ± 0.07 mm ventral to bregma; N=12 experiments). Mean ± s.e.m. in vitro ACh recovery of probes used to deliver hypocretin-1 (6.0 ± 0.2%) and hypocretin-2 (6.4 ± 0.3%) also was not significantly different. These measures provided important controls indicating that differences reported below (Figs. 5 and 6) in the magnitude of the ACh response to equimolar concentrations of hypocretin-1 and hypocretin-2 were not artifacts due to differences in intrapontine site of hypocretin delivery or differences in amounts of ACh recovered by the dialysis probes.

Figure 5 summarizes ACh release during Ringer's (control) dialysis and during dialysis with four concentrations of hypocretin-1 (Fig. 5A-D) and hypocretin-2 (Fig. 5E-H). Each bar represents mean ± s.e.m. ACh release obtained from three experiments. Variability among the five Ringer's control ACh samples was similar for all experiments. Dialysis with 0.1 μM hypocretin-1 (Fig. 5A) or 0.1 μM hypocretin-2 (Fig. 5E) did not alter ACh release. Figure 5B shows that 1 μM hypocretin-1 significantly increased ACh release during the second 15 min sampling period. In contrast, 1 μM hypocretin-2 did not increase ACh release (Fig. 5F). Dialysis with 10 and 100 μM hypocretin-1 (Fig. 5C and 5D) caused significant increases in ACh release. In contrast to Fig. 5E, 5F, and 5G, only the 100 μM concentration of hypocretin-2 significantly increased ACh release (Fig. 5H). There was no significant difference between

mean ± s.e.m. basal (Ringer's) ACh levels for experiments delivering hypocretin-1 (0.141 ± 0.006 pmol/15 min, Fig. 5A-D) and experiments delivering hypocretin 2 (0.142 ± 0.005 pmol/15 min, Fig. 5E-H). This finding supports the interpretation that differences in the magnitude of the ACh response to equimolar concentrations of hypocretin-1 and hypocretin-2 were not artifacts resulting from differences in basal levels of ACh release.

Figure 6 shows the concentration response curves for hypocretin-1- and hypocretin-2-stimulated ACh release. Two-way ANOVA was based on 119 dialysis samples, accounted for as follows: (5 samples per peptide concentration x 4 peptide concentrations x 2 peptides x 3 rats per peptide concentration) minus one missing value. Two-way ANOVA revealed a significant drug main effect ($F=10.1$; $df=1,111$; $p=0.0019$), a significant concentration main effect ($F=28.9$; $df=3,111$; $p<0.0001$), and no significant interaction. A post hoc Bonferroni test revealed that 10 and 100 μM hypocretin-1 caused a significantly ($p<0.05$) greater increase in ACh release than respective, equimolar concentrations of hypocretin-2.

Discussion

This study used G protein activation and ACh release as functional measures to elucidate mechanisms of hypocretin signaling in rat PnO. Hypocretin-1-stimulated G protein activation was significantly decreased by pertussis toxin, providing the first demonstration that hypocretin receptors in the PnO are pertussis toxin-sensitive. This finding suggests that some hypocretin receptors in rat PnO couple to inhibitory G proteins. Pertussis toxin did not inhibit hypocretin-1-induced ACh release, implying that hypocretin stimulates ACh release in rat PnO via receptors coupled to non-inhibitory G proteins. Concentration response studies using hypocretin-1 and hypocretin-2 revealed that both hypocretin receptor subtypes modulate ACh release in the PnO. The demonstration that hypocretin signaling in the PnO involves both pertussis toxin-sensitive and pertussis toxin-insensitive G proteins indicates, for the first time, that hypocretin receptors in rat PnO couple to both inhibitory and stimulatory G proteins. The results are consistent with the interpretation that one mechanism by which hypocretin promotes arousal is by increasing ACh release in the pontine reticular formation.

Hypocretin receptors activate pertussis toxin-sensitive G proteins in rat PnO. In vitro [^{35}S]GTPγS autoradiography has been used successfully to quantify the functional activity of many different G protein coupled receptors (Sóvágó et al., 2001). Agonist activated [^{35}S]GTPγS binding in brain is thought to preferentially label inhibitory (Gi/o, Gz), rather than stimulatory (Gs, Gq) G proteins (Sóvágó et al., 2001; Harrison and Traynor, 2003; Laitinen, 2004). Pertussis toxin selectively inactivates Gi/o proteins and pertussis toxin has been shown to be effective following microinjection into rat striatum (van der Ploeg et al., 1991), ventral tegmental area (Gronier and Rasmussen, 1999), substantia nigra compacta (Gronier and

Rasmussen, 1999), and hippocampus (Tzavara et al., 2003). The present finding that PnO microinjection of pertussis toxin decreased hypocretin-1-stimulated [^{35}S]GTPγS binding in the PnO (Fig.1B) is the first direct evidence that hypocretin activates inhibitory G proteins in rat pontine reticular formation. This result is consistent with the interpretation that some hypocretin receptors in rat PnO couple to Gi/o proteins. An alternative explanation is that PnO hypocretin receptors indirectly activate Gi/o proteins via G protein cross talk (Vazquez-Prado et al., 2003) or heterodimerization of hypocretin receptors (Karteris and Randeva, 2003) with other Gi/o protein coupled receptors (Devi, 2001).

To further test the interpretation that hypocretin-1 activates Gi/o proteins in rat PnO, the effects of pertussis toxin on DAMGO-stimulated [^{35}S]GTPγS binding also were quantified. The mu opioid agonist DAMGO was used as a positive control because mu opioid receptors couple exclusively to Gi/o proteins (Birnbaumer et al., 1990). DAMGO-stimulated [^{35}S]GTPγS binding was significantly reduced by pretreatment with pertussis toxin (Fig. 1C, compare filled bars), confirming that microinjection of pertussis toxin effectively inactivated Gi/o proteins in the PnO. DAMGO-stimulated [^{35}S]GTPγS binding was not completely eliminated by pretreatment with pertussis toxin (Fig. 1C: PTX injection, hatched versus filled bar, †). A higher concentration of pertussis toxin than was used in the present study may be required to eliminate the remaining DAMGO-stimulated G protein activation. Alternatively, the remaining DAMGO-stimulated G protein activation may have resulted from activating mu opioid receptors that couple to pertussis toxin-insensitive inhibitory G proteins (Gz) (Ho and Wong, 2001).

Additional control experiments were performed by microinjecting the vehicle solution for pertussis toxin into the PnO before [^{35}S]GTPγS autoradiography (Fig. 1D). Compared to no injection, vehicle injection did not alter specific [^{35}S]GTPγS binding levels for basal (Fig. 1E,

JPET Fast Forward. Published on December 13, 2005 as DOI: 10.1124/jpet.105.097071
This article has not been copyedited and formatted. The final version may differ from this version.

compare hatched bars), hypocretin-1 (Fig. 1E, compare solid bars), and DAMGO (Fig. 1F, compare solid bars) treatment conditions. These data demonstrate that vehicle injection did not alter [^{35}S]GTPγS binding, and confirm that the block of DAMGO- and hypocretin-1-stimulated [^{35}S]GTPγS binding was due to the pharmacological actions of pertussis toxin. Hypocretin-stimulated [^{35}S]GTPγS binding in rat pons is known to be a receptor mediated response because it is concentration dependent and blocked by specific hypocretin receptor antagonists (Shiba et al., 2002; Bernard et al., 2003; Bernard et al., 2005). Therefore, the Fig. 1 results support the conclusion that some hypocretin receptors in rat PnO couple to pertussis toxin-sensitive inhibitory G proteins. This conclusion is consistent with in vitro electrophysiological data showing that hypocretin-induced alterations in cell excitability are inhibited by pertussis toxin (Hoang et al., 2003; van den Top et al., 2003; Zhu et al., 2003; Holmqvist et al., 2005).

Hypocretin-1-stimulated ACh release in the PnO is mediated by pertussis toxin-insensitive G proteins. The present study aimed to determine if one mechanism by which hypocretin modulates ACh release includes activation of pertussis toxin-sensitive G proteins in rat PnO. Using the same protocol shown to be effective for blocking hypocretin-1-stimulated G protein activation (Fig. 1), pertussis toxin was microinjected into the PnO 48 h before dialysis administration of hypocretin-1 or SPA (Fig. 2). Positive control experiments utilized the adenosine A_1 receptor agonist SPA, which is known to activate pertussis toxin-sensitive G proteins (Ribeiro et al., 2003) and inhibit ACh release (Tanase et al., 2003). Pertussis toxin blocked the SPA-induced decrease in ACh release (Fig. 3B), confirming that Gi/o proteins were inactivated. In contrast, the hypocretin-1-induced increase in ACh release was not blocked by pertussis toxin (Fig. 3A), suggesting that hypocretin-1-stimulated ACh release is mediated by

non-inhibitory G proteins. Additional control experiments established that ACh release was not altered due to vehicle microinjection (Fig. 3).

The conclusion that hypocretin receptors modulating ACh release in PnO couple to stimulatory G proteins is consistent with the neuroexcitatory activity of hypocretin (de Lecea et al., 1998). Hypocretin receptors also have been suggested to signal through Gq proteins (van den Pol et al., 1998; Zhu et al., 2003), which are known to stimulate phosphoinositol turnover and increase intracellular Ca^{2+}. Hypocretin-1-stimulated calcium release in Chinese hamster ovary cell lines (Smart et al., 1999) and in hypothalamic neurons (van den Pol et al., 1998) involves phospholipase C and/or protein kinase C. Alternatively, hypocretin-1 could stimulate ACh release via pertussis toxin-insensitive inhibitory G proteins (Knott et al., 1993). However, the present observation that pertussis toxin inhibits hypocretin-1-stimulated G protein activation (Fig. 1) suggests that in rat PnO, some hypocretin receptors couple to inhibitory G proteins that are indeed pertussis toxin-sensitive. In addition, the Fig. 3 results show for the first time that hypocretin-1-stimulated ACh release in the PnO involves activation of pertussis toxin-insensitive G proteins.

Both hypocretin receptor subtypes modulate ACh release in rat PnO. The discovery that hypocretin-1 stimulates ACh release via non-inhibitory G proteins encouraged further studies aiming to reveal the hypocretin receptor subtype modulating ACh release in the PnO (Fig. 4). Hypocretin-1 and hypocretin-2 each caused a concentration dependent increase in ACh release (Figs. 5 and 6). The two peptides showed only about a two-fold difference in EC_{50} values (Fig. 6), consistent with the interpretation that hcrt-r2 modulates ACh release in the PnO (Sakurai et al., 1998; Smart et al., 1999; Smart et al., 2001). At concentrations of 10 μM and 100

μM, hypocretin-1 caused a significantly greater increase in ACh release than hypocretin-2 (Fig. 6), suggesting that hcrt-r1 also may be involved in modulating PnO ACh release. Both hypocretin receptor subtypes are expressed in rat PnO (Greco and Shiromani, 2001). Thus, these data provide novel evidence that ACh release in rat PnO is modulated by hcrt-r2 and hcrt-r1.

Functional Implications. One new finding presented here is that rat PnO contains a population of hypocretin receptors that activate pertussis toxin sensitive G proteins (Fig. 1). The function served by hypocretinergic activation of putatively inhibitory G proteins is unknown. The present study also showed, for the first time, that hypocretin-1 causes a pertussis toxin insensitive increase in ACh release within the PnO (Fig. 3), and that both peptides evoke a concentration dependent increase in PnO ACh release (Fig. 6). These data provide the first functional evidence that hypocretin receptors in rat PnO activate stimulatory G proteins. Increasing ACh release in PnO may be one mechanism by which hypocretin promotes brain activation. Cholinergic transmission in the pontine reticular formation participates in generating the cortical activation characteristic of wakefulness and rapid eye movement sleep (Lydic and Baghdoyan, 2005), and microinjection of hypocretin-1 into cat pontine reticular formation can trigger REM sleep (Xi et al., 2002). Interactions between cholinergic and GABAergic transmission in the pontine reticular formation promote wakefulness, particularly when GABAergic transmission is enhanced (Xi et al., 2004). Most recently, hypocretin-1 has been shown to cause a concentration dependent increase in PnO GABA levels (Soto-Calderon et al., 2005). Taken together, these findings are consistent with the interpretation that hypocretin promotes arousal, in part, by increasing ACh release in PnO.

Acknowledgements

For expert assistance the authors thank S. Jiang and M.A. Norat of the Department of Anesthesiology, and K. Welch of the University of Michigan Center for Statistical Analysis and Research.

References

Bernard R, Lydic R and Baghdoyan HA (2003) Hypocretin-1 causes G protein activation and increases ACh release in rat pons. *Eur J Neurosci* **18**:1775-1785.

Bernard R, Lydic R and Baghdoyan HA (2005) Hypocretin receptor-activated G proteins revealed by [^{35}S]GTPS autoradiography, in *The Orexin/Hypocretin System: Physiology and Pathophysiology* (Nishino S and Sakurai T eds) pp 83-96, Humana Press Inc., Totowa, NJ.

Birnbaumer L, Abramowitz J and Brown AM (1990) Receptor-effector coupling by G proteins. *Biochim Biophys Acta* **1031**:163-224.

Carty D (1994) Pertussis toxin-catalyzed ADP-ribosylation of G proteins. *Methods Enzymol* **237**:63-70.

Chemelli RM, Willie JT, Sinton CM, Elmquist JK, Scammell T, Lee C, Richardson JA, Williams SC, Xiong Y, Kisanuki Y, Fitch TE, Nakazato M, Hammer RE, Saper CB and Yanagisawa M (1999) Narcolepsy in *orexin* knockout mice: molecular genetics of sleep regulation. *Cell* **98**:437-451.

de Lecea L, Kilduff TS, Peyron C, Gao X, Foye PE, Danielson PE, Fukuhara C, Battenberg EL, Gautvik VT, Bartlett FS, 2nd, Frankel WN, van den Pol AN, Bloom FE, Gautvik KM and Sutcliffe JG (1998) The hypocretins: hypothalamus-specific peptides with neuroexcitatory activity. *Proc Natl Acad Sci USA* **95**:322-327.

Devi LA (2001) Heterodimerization of G-protein-coupled receptors: pharmacology, signaling and trafficking. *Trends Pharm Sciences* **22**:532-537.

Greco MA and Shiromani PJ (2001) Hypocretin receptor protein and mRNA expression in the dorsolateral pons of rats. *Brain Res Mol Brain Res* **88**:176-182.

Gronier B and Rasmussen K (1999) Pertussis toxin treatment differentially affects cholinergic and dopaminergic receptor stimulation of midbrain dopaminergic neurons. *Neuropharmacology* **38**:1903-1912.

Harrison C and Traynor JR (2003) The [^{35}S]GTPγS binding assay: approaches and applications in pharmacology. *Life Sci* **74**:489-508.

Ho MK and Wong YK (2001) G(z) signaling: emerging divergence from G(i) signaling. *Oncogene* **20**:1615-1625.

Hoang QV, Bajic D, Yanagisawa M, Nakajima S and Nakajima Y (2003) Effects of orexin (hypocretin) on GIRK channels. *J Neurophysiol* **90**:693-702.

Holmqvist T, Johansson L, Ostman M, Ammoun S, Akerman KEO and Kukkonen JP (2005) OX1 orexin receptors couple to adenylyl cyclase regulation via multiple mechanisms. *J Biol Chem* **280**:6570-6579.

Karteris E and Randeva HS (2003) Orexin receptors and G-protein coupling: evidence for another "promiscuous" seven transmembrane domain receptor. *J Pharmacol Sci* **93**:126-128.

Kilduff TS and Peyron C (2000) The hypocretin/orexin ligand-receptor system: implications for sleep and sleep disorders. *Trends Neurosci* **23**:359-365.

Knott C, Maguire JJ, Moratalla R and Bowery NG (1993) Regional effects of pertussis toxin in vivo and in vitro on $GABA_B$ receptor binding in rat brain. *Neuroscience* **52**:73-81.

Kukkonen JP, Holmqvist T, Ammoun S and Åkerman KE (2002) Functions of the orexinergic/hypocretinergic system. *Am J Physiol Cell Physiol* **283**:C1567-C1591.

Laitinen JT (2004) [^{35}S]GTPγS autoradiography: a powerful functional approach with expanding potential for neuropharmacological studies on receptors coupled to Gi family of G proteins. *Curr Neuropharmacol* **2**:191-206.

Lee MG, Hassani OK and Jones BE (2005) Discharge of identified orexin/hypocretin neurons across the sleep-waking cycle. *J Neurosci* **25**:6716-6720.

Lin L, Faraco J, Li R, Kadotani H, Rogers W, Lin X, Qiu X, de Jong PJ, Nishino S and Mignot E (1999) The sleep disorder canine narcolepsy is caused by a mutation in the hypocretin (orexin) receptor 2 gene. *Cell* **98**:365-376.

Lydic R and Baghdoyan HA (2005) Sleep, anesthesiology, and the neurobiology of arousal state control. *Anesthesiology* **103**:1268-1295.

Mileykovskiy BY, Kiyashchenko LI and Siegel JM (2005) Behavioral correlates of activity in identified hyocretin/orexin neurons. *Neuron* **46**:787-798.

Nishino S, Ripley B, Overeem S, Lammers GJ and Mignot E (2000) Hypocretin (orexin) deficiency in human narcolepsy. *Lancet* **355**:39-40.

Paxinos G and Watson C (1998) *The Rat Brain in Stereotaxic Coordinates, 4th Edition.* Academic Press, New York.

Peyron C, Tighe DK, van den Pol AN, de Lecea L, Heller HC, Sutcliffe JG and Kilduff TS (1998) Neurons containing hypocretin (orexin) project to multiple neuronal systems. *J Neurosci* **18**:9996-10015.

Ribeiro JA, Sebastiao AM and de Mendonca A (2003) Adenosine receptors in the nervous system: pathophysiological implications. *Prog Neurobiol* **68**:377-392.

Sakurai T, Amemiya A, Ishii M, Matsuzaki I, Chemelli RM, Tanaka H, Williams SC, Richardson JA, Kozlowski GP, Wilson S, Arch JR, Buckingham RE, Haynes AC, Carr SA, Annan RS, McNulty DE, Liu WS, Terrett JA, Elshourbagy NA, Bergsma DJ and Yanagisawa M (1998) Orexins and orexin receptors: a family of hypothalamic neuropeptides and G protein-coupled receptors that regulate feeding behavior. *Cell* **92**:573-585.

Shiba T, Ozu M, Yoshida Y, Mignot E and Nishino S (2002) Hypocretin stimulates [^{35}S]GTPγS binding in hcrtr 2-transfected cell lines and in brain homogenate. *Biochem Biophys Res Com* **294**:615-620.

Smart D and Jerman JC (2002) The physiology and pharmacology of the orexins. *Pharmacol Ther* **94**:51-61.

Smart D, Jerman JC, Brough SJ, Rushton SL, Murdock PR, Jewitt F, Elshourbagy, Ellis CE, Middlemiss DN and Brown F (1999) Characterization of recombinant human orexin receptor pharmacology in a Chinese hamster ovary cell-line using FLIPR. *Br J Pharmacol* **128**:1-3.

Smart D, Sabido-David C, Brough SJ, Jewitt F, Johns A, Porter RA and Jerman JC (2001) SB-334867-A: the first selective orexin-1 receptor antagonist. *Br J Pharmacol* **132**:1179-1182.

Soto-Calderon H, Lydic R and Baghdoyan HA (2005) GABA levels are increased in the pontine reticular nucleus, oral part (PnO) of anesthetized rat by dialysis administration of hypocretin-1 (orexin A). *Sleep* **28 (Abstr Suppl)**:0036.

Sóvágó J, Dupuis DS and Gulyás B (2001) An overview on functional receptor autoradiography using [^{35}S]GTPγS autoradiography. *Brain Res Rev* **38**:148-164.

Tanase D, Baghdoyan HA and Lydic R (2003) Dialysis delivery of an adenosine A_1 receptor agonist to the pontine reticular formation decreases acetylcholine release and increases anesthesia recovery time. *Anesthesiology* **98**:912-920.

Thannickal TC, Moore RY, Nienhuis R, Ramanathan L, Gulyani S, Aldrich M, Comford M and Siegel JM (2000) Reduced number of hypocretin neurons in human narcolepsy. *Neuron* **27**:469-474.

Tzavara ET, Wade M and Nomikos GG (2003) Biphasic effects of cannabinoids on acetylcholine release in the hippocampus: site and mechanism of action. *J Neurosci* **23**:9374-9384.

van den Pol AN, Gao XB, Obrietan K, Kilduff TS and Belousov AB (1998) Presynaptic and postsynaptic actions and modulation of neuroendocrine neurons by a new hypothalamic peptide, hypocretin/orexin. *J Neurosci* **18**:7962-7971.

van den Top M, Nolan MF, Lee K, Richardson PJ, Buijs RM, Davies CH and Spanswick D (2003) Orexins induce increased excitability and synchronisation of rat sympathetic preganglionic neurones. *J Physiol* **549.3**:809-821.

van der Ploeg I, Cintra A, Altiok N, Askeloef P, Fuxe K and Fredholm BB (1991) Limited distribution of pertussis toxin in rat brain after injection into the lateral cerebral ventricles. *Neuroscience* **44**:205-214.

Vazquez-Prado J, Casas-Gonzalez P and Garcia-Sainz JA (2003) G protein-coupled receptor cross talk: pivotal roles of protein phosphorylation and protein-protein interaction. *Cell Signal* **15**:549-557.

Xi M-C, Fung SJ, Yamuy J, Morales FR and Chase MH (2002) Induction of active (REM) sleep by microinjection of hypocretin into the nucleus pontis oralis of the cat. *J Neurophysiol* **87**:2880-2888.

Xi M-C, Morales FR and Chase MH (2004) Interactions between GABAergic and cholinergic processes in the nucleus pontis oralis: neuronal mechanisms controlling active (rapid eye movement) sleep and wakefulness. *J Neurosci* **24**:10670-10678.

Zhu Y, Miwa Y, Yamanaka A, Yada T, Shibahara M, Abe Y, Sakurai T and Goto K (2003) Orexin receptor type-1 couples exclusively to pertussis toxin-insensitive G-proteins, while orexin receptor type-2 couples to both pertussis toxin-sensitive and -insensitive G-proteins. *J Pharmacol Sci* **92**:259-266.

Footnotes

a) Supported by National Institutes of Health grants MH45361, HL57120, HL40881, HL65272, and by the Department of Anesthesiology, University of Michigan.

b) Address reprint requests to:

Helen A. Baghdoyan, Ph.D.

University of Michigan

Department of Anesthesiology

7433 Medical Sciences Building I

1150 West Medical Center Drive

Ann Arbor, Michigan 48109-0615

Voice: (734) 647-7831

Fax: (734) 764-9332

Email: helenb@umich.edu

c) RB, RL, HAB, Department of Anesthesiology, University of Michigan

RB, HAB, Department of Pharmacology, University of Michigan

Figure Legends

Figure 1

Pretreatment with pertussis toxin inhibited hypocretin-1-stimulated G protein activation. Coronal brainstem plates were modified from a rat brain atlas (Paxinos and Watson, 1998). Statistically significant differences between in vitro [^{35}S]GTPγS binding conditions are indicated by crosses ($p<0.05$) or asterisks ($p<0.01$). A, pertussis toxin was delivered unilaterally to the pontine reticular nucleus, oral part (PnO) via microinjection prior to performing in vitro autoradiography. B, Hypocretin-1 (Hcrt-1) increased [^{35}S]GTPγS binding on the non-injected (control) side of the PnO, but not on the pertussis toxin-injected side. This finding indicates that hypocretin-1 activates pertussis toxin-sensitive G proteins in rat PnO. C, Positive control experiments showed that DAMGO increased [^{35}S]GTPγS binding in the non-injected PnO, and that pertussis toxin significantly reduced DAMGO-stimulated G protein activation. This finding demonstrates that pertussis toxin effectively inactivated G proteins in the PnO. D, as an additional control, vehicle solution was unilaterally microinjected into the PnO before in vitro autoradiography. E, Vehicle (VEH) microinjection did not inhibit the hypocretin-1-induced increase in [^{35}S]GTPγS binding. F, vehicle microinjection did not inhibit the DAMGO-induced increase in [^{35}S]GTPγS binding.

Figure 2

Microdialysis sites were histologically localized to the pontine reticular formation, oral part (PnO). Cylinders indicating dialysis membranes are drawn to scale and are plotted on coronal atlas plates (Paxinos and Watson, 1998) spanning from bregma –7.80 mm to –8.30 mm.

Figure 3

Hypocretin-1-stimulated ACh release in the PnO was not inhibited by microinjection of pertussis toxin (PTX) or vehicle (VEH). A, the hypocretin-1 (hcrt-1)-stimulated increase in ACh release was not blocked by pretreating the PnO with pertussis toxin. B, positive control experiments demonstrated that the SPA-induced decrease in ACh release was blocked by pertussis toxin pretreatment. Considered together, the results illustrated by parts A and B indicate that hypocretin-1 increases ACh release by activating pertussis toxin-insensitive G proteins in rat PnO.

Figure 4

Sites for dialysis administration of hypocretin-1 and hypocretin-2 were localized to the pontine reticular nucleus, oral part (PnO). Coronal plates spanning from bregma -7.80 mm to -8.72 mm were modified from a rat brain atlas (Paxinos and Watson, 1998). Cylinders indicating dialysis membranes are drawn to scale. A, digitized images of cresyl violet stained coronal brainstem sections show representative dialysis sites from two rats. Arrows indicate the deepest portion of the dialysis membranes. B, dialysis sites from experiments that examined the effect of hypocretin-1 on ACh release were all within the PnO. Twelve rats (3 per concentration) were used for these studies. Each rat was used only once. C, dialysis sites for determining the effects of hypocretin-2 on ACh release were confirmed to be in the PnO. Twelve rats (3 per concentration) were used for these studies. Each rat was used only once.

Figure 5

Hypocretin-1 and hypocretin-2 caused concentration dependent increases in ACh release. Each of the eight graphs shows average ACh release from three experiments per concentration, plotted in sequential 15 min bins during dialysis with Ringer's solution (control) followed by hypocretin-1 (A-D) or hypocretin-2 (E-H). Asterisks indicate samples in which ACh was significantly ($p<0.05$) increased over mean Ringer's levels. Concentration dependence supports the interpretation that the increase in ACh release caused by hypocretin is modulated by hypocretin receptors localized to rat pontine reticular formation.

Figure 6

Concentration response curves for ACh release stimulated by hypocretin-1 and hypocretin-2. Data were obtained from three experiments per concentration for each peptide. The coefficients of determination (r^2) indicated that 99.9 and 100% of the variability in ACh was accounted for by the concentration of hypocretin-1 and hypocretin-2, respectively. EC_{50} values for increasing ACh were 4.7 μM for hypocretin-1 and 11.0 μM for hypocretin-2. Asterisks indicate that at concentrations of 10 and 100 μM, hypocretin-1 caused a significantly ($p<0.05$) greater increase in ACh release than hypocretin-2.

JPET Fast Forward. Published on December 13, 2005 as DOI: 10.1124/jpet.105.097071
This article has not been copyedited and formatted. The final version may differ from this version.

Figure 1

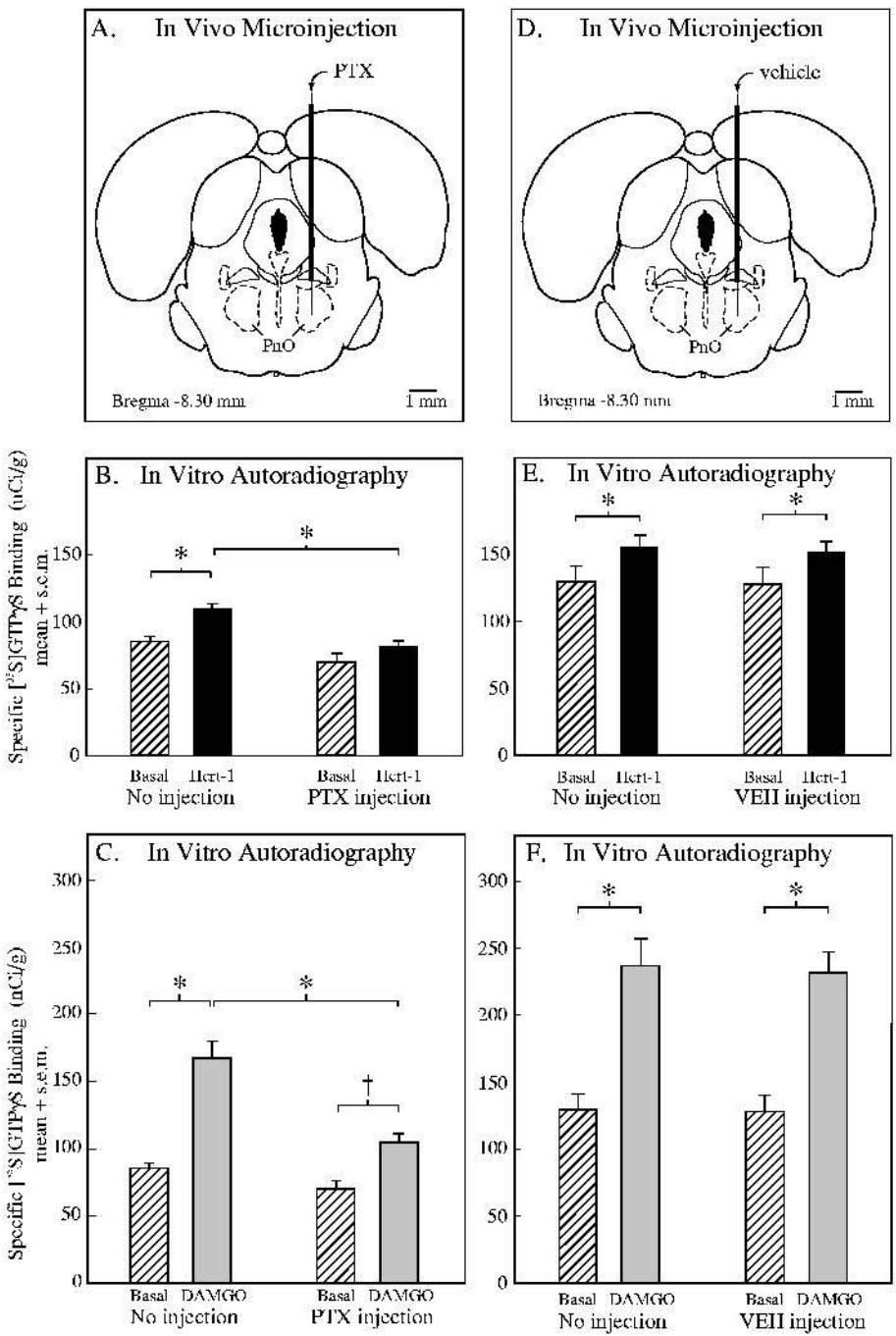

JPET Fast Forward. Published on December 13, 2005 as DOI: 10.1124/jpet.105.097071
This article has not been copyedited and formatted. The final version may differ from this version.

Figure 2

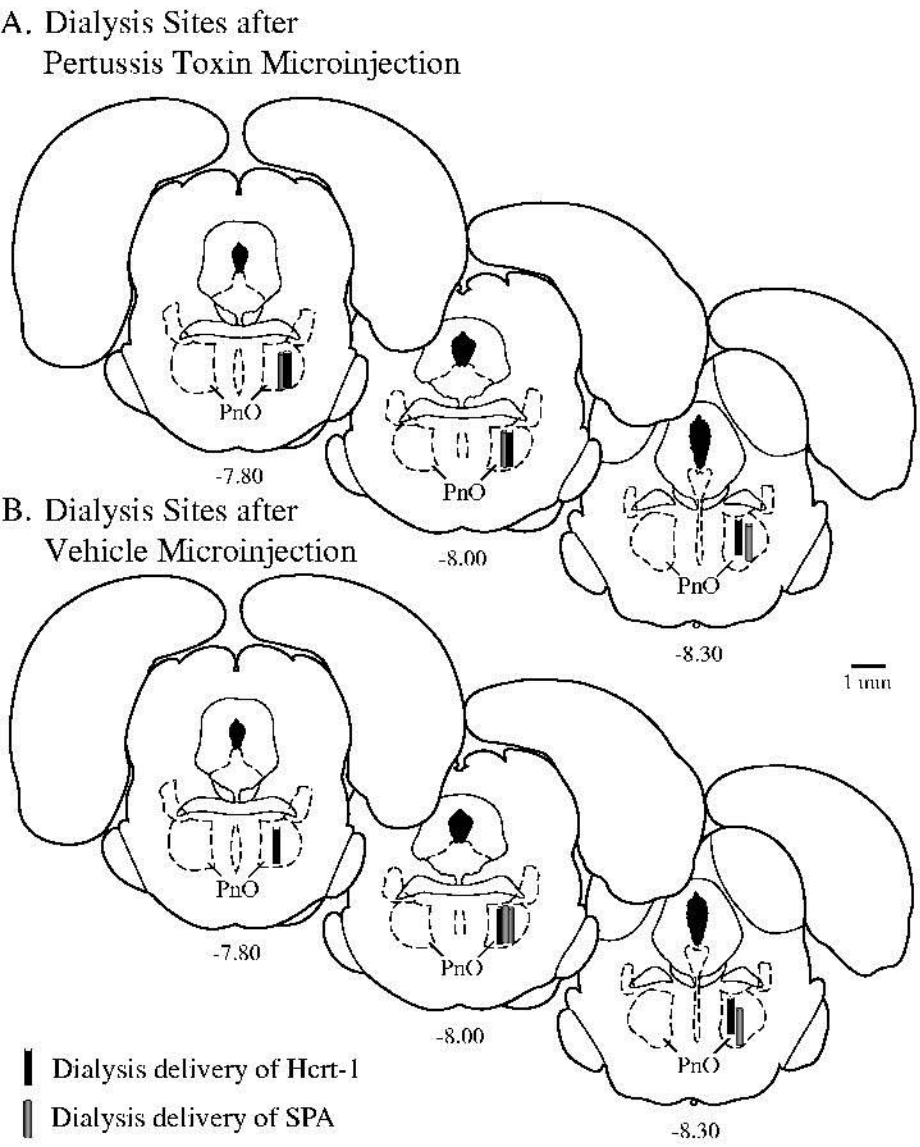

JPET Fast Forward. Published on December 13, 2005 as DOI: 10.1124/jpet.105.097071
This article has not been copyedited and formatted. The final version may differ from this version.

Figure 3

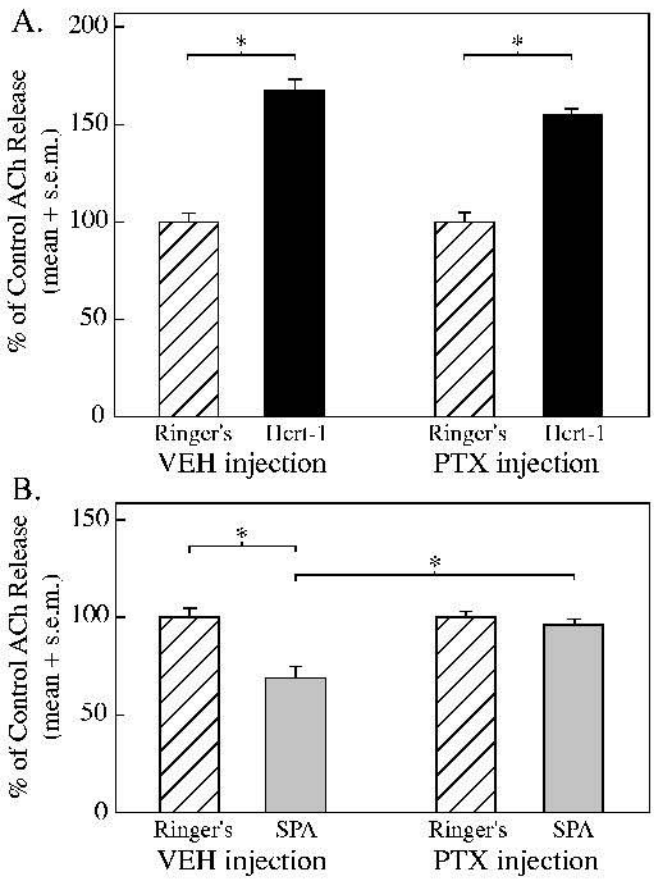

JPET Fast Forward. Published on December 13, 2005 as DOI: 10.1124/jpet.105.097071
This article has not been copyedited and formatted. The final version may differ from this version.

Figure 4

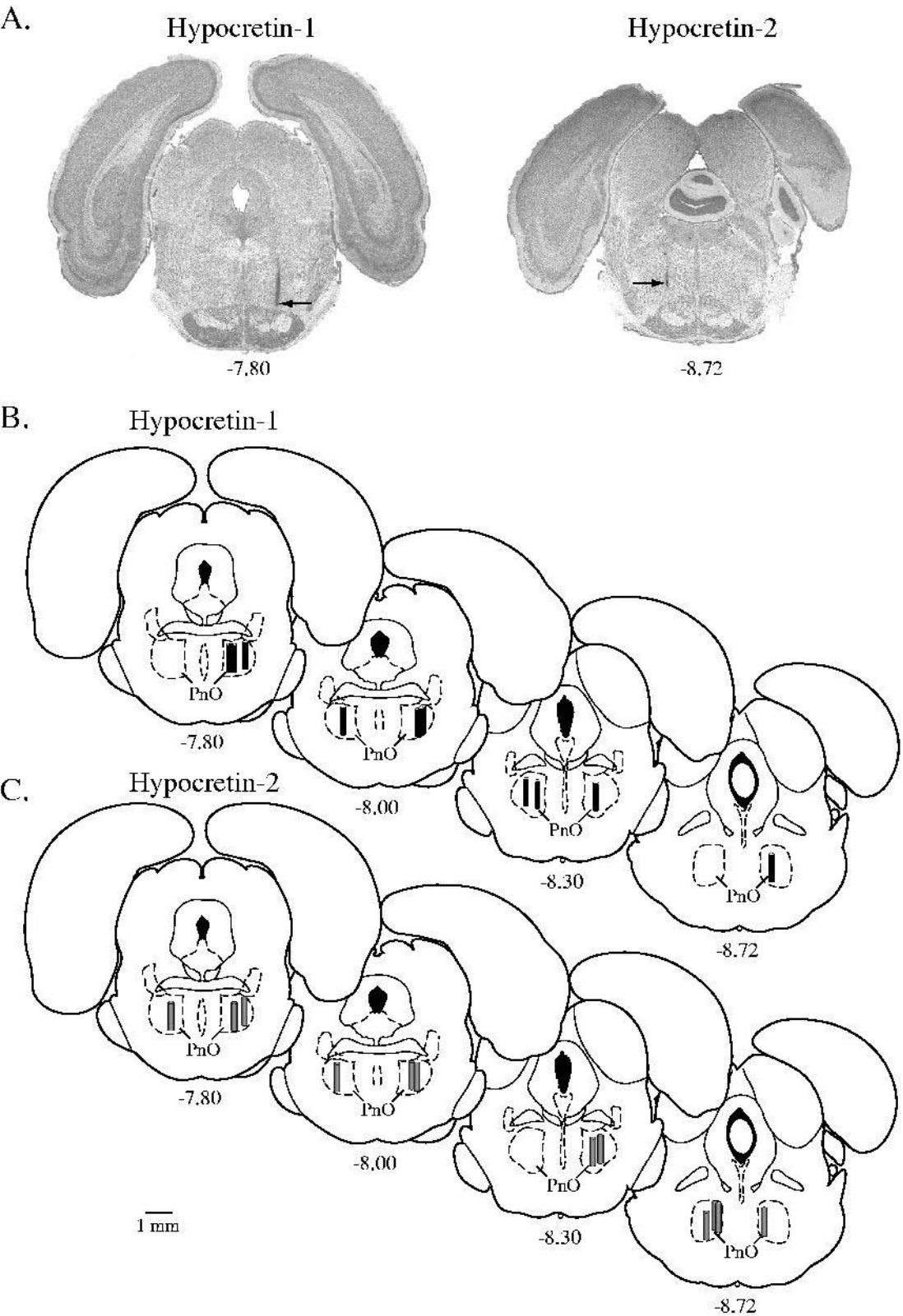

JPET Fast Forward. Published on December 13, 2005 as DOI: 10.1124/jpet.105.097071
This article has not been copyedited and formatted. The final version may differ from this version.

Figure 5

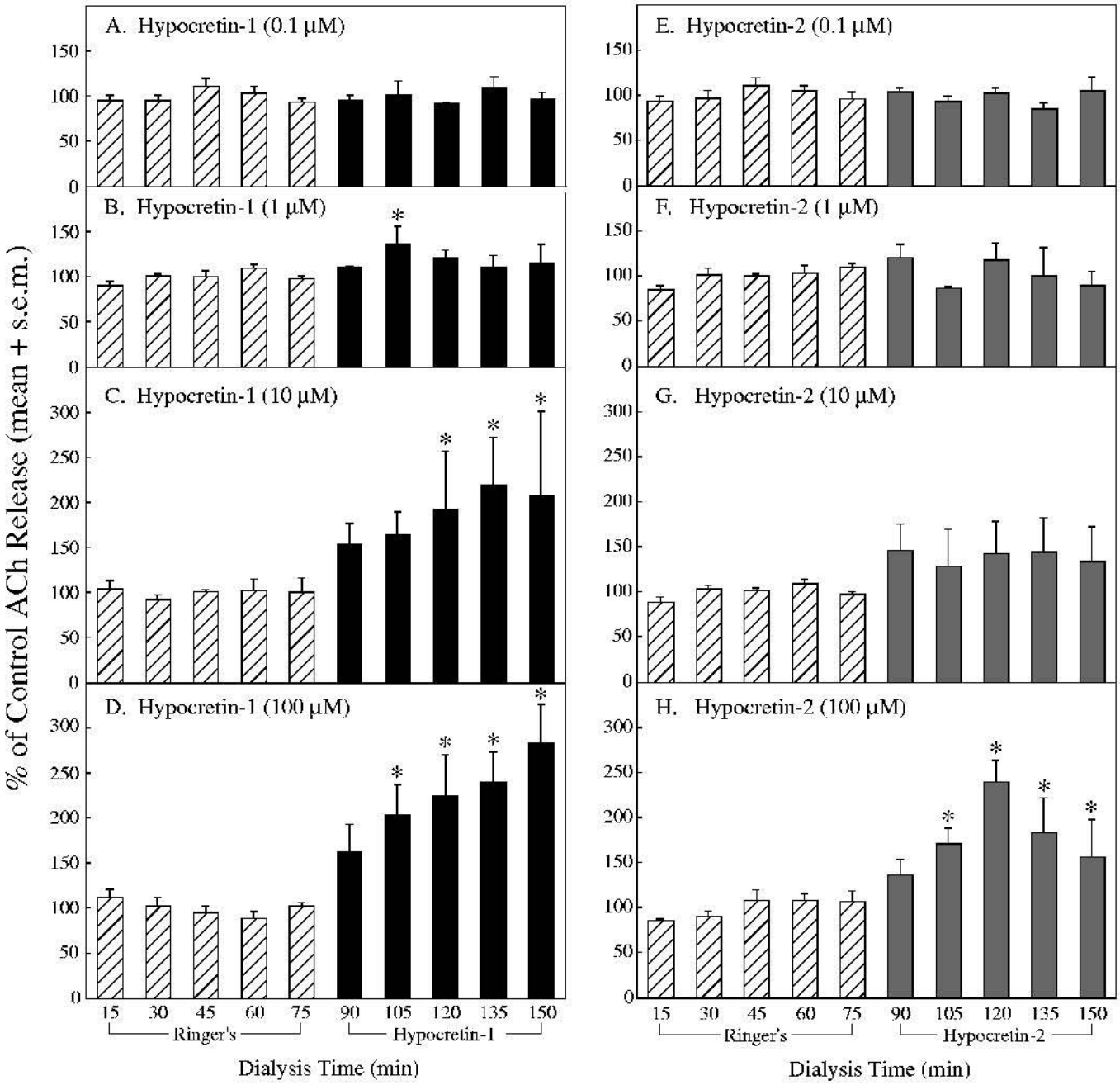

JPET Fast Forward. Published on December 13, 2005 as DOI: 10.1124/jpet.105.097071
This article has not been copyedited and formatted. The final version may differ from this version.

Figure 6